NUCLEAR INSTRUMENTS AND METHODS 65 (1968) 8–25; © NORTH-HOLLAND PUBLISHING CO.

CALIBRATION OF AN ORGANIC SCINTILLATOR FOR NEUTRON SPECTROMETRY*

V. V. VERBINSKI†, W. R. BURRUS+, T. A. LOVE, W. ZOBEL and N. W. HILL

Oak Ridge National Laboratory, Oak Ridge, Tennessee, U.S.A.

R. TEXTOR

Computing Technology Center, Oak Ridge Gaseous Diffusion Plant, Oak Ridge, Tennessee, U.S.A.

Received 13 May 1968

The absolute differential efficiency of a 4.60- × 4.65-cm-dia. liquid organic scintillator, NE-213, was determined for nearly monoenergetic neutrons at 20 energies between 0.2 and 22 MeV incident on the curved side of the detector. These calibrations are shown to apply to an NE-211 scintillator as well. A 5-MeV Van de Graaff generator provided 2-nsec pulses of neutrons by means of T(p,n)^{3}He, D(d,n)^{3}He (gas target), and T(d,n)^{4}He reactions. With the aid of time-of-flight techniques and pulse-shape discrimination to eliminate spurious neutron and gamma-ray events, reliable pulse-height spectra were obtained for monoenergetic neutrons. The spectra were normalized to Monte Carlo calculations of absolute differential efficiency by utilizing the proton-recoil plateau. The accuracy of the Monte Carlo calculation was verified in the region of the proton-recoil plateau by absolute experimental calibrations carried out at neutron energies of 2.66 and 14.43 MeV and by using a scintillator geometry more suitable for such tests.

1. Introduction

The present calibration combines the best features of a series of measurements and of Monte Carlo[1]) calculations of pulse-height spectra for monoenergetic neutrons incident on an organic liquid scintillator. The calculations provide accurate differential efficiencies at large pulse heights, where hydrogen collisions are predominant and where neutron reactions with carbon nuclei do not contribute directly. Consequently, normalization of the measured pulse-height spectra to calculations at the upper end of each spectrum converts the accurately measured spectral shapes to absolute differential efficiencies that are more accurate than those that could be obtained by measurement or calculation alone. It would be desirable, however, to perfect the calculations to produce results with comparable reliability, so that calculations could easily be made for other scintillator geometries. The calibrations presented here should prove useful in improving the input data for existing Monte Carlo response calculations, particularly cross sections of various neutron reactions with carbon, kinetic energy and angular distributions for each possible reaction product, and the light yields as a function of kinetic energy.

The measurements were made with the use of a pulse-shape discriminator circuit to reject gamma-ray events, and the calculations correspondingly ignored gamma-ray production following neutron reactions. The pulse-shape discrimination circuit, which is described in more detail in a related paper[2]), is a variant of one of Forte's circuits[3]). When used with high-gain photomultiplier tubes operated with the proper amount of saturation at the anode, it worked well over a pulse-height range of 150:1 without correction and of 400:1 with correction for efficiency rolloff at low pulse heights. The correction functions were obtained with the associated-particle method described in section 5, a method that is generally useful in evaluating pulse-shape discrimination circuits.

The subject matter of the remaining sections is as follows: section 2: the choice of scintillators, the properties, and the optical coupling; section 3: the procedure for preparing the Monte Carlo calculations for direct comparison to the measurements; section 4: the accuracy and limitations of the calculations and some supporting experimental checks of the calculations; section 5: the experimental arrangement and apparatus for calibrating the detector; section 6: the methods of gain checks and data taking; section 7: the data-handling and the final results; and section 8: several methods of utilizing these calibrations for neutron spectroscopy.

2. The scintillators

A small, 4.60- by 4.65-cm-dia., cylinder of NE-213 scintillator was chosen because it offers a good compromise between efficiency and resolutions. NE-213 has an enhanced emission of delayed light which gives it

* Research jointly sponsored by the National Aeronautics and Space Administration and the Defense Atomic Support Agency and performed under subcontract for the Oak Ridge National Laboratory operated by Union Carbide Corporation under contract with the U. S. Atomic Energy Commission.

† Present address: Gulf General Atomic, P.O. Box 608, San Diego, California.

+ Present address: Tennecomp, Inc., P.O. Box J, Oak Ridge, Tennessee.

good pulse-shape-discrimination capabilities. Since NE-213 is noncrystalline, it is isotropic in response to neutrons and is not sensitive to mechanical or thermal shock. Carbon recoils and alpha particles from 14-MeV neutrons on NE-213 and its counterpart NE-211 produce only about half the pulse height that is produced with stilbene scintillators, when normalizing to the largest hydrogen-recoil pulses. The pulses from carbon reactions can therefore be more easily biased out in NE-211 and NE-213 when desired.

The NE-213 scintillator* used for this work is made with xylene, activators, and POPOP as a wave shifter. Naphthalene is added to enhance the slow component of light emission. This is important to achieving a good pulse-shape-discrimination capability[2,3]). The scintillator was glass-encapsulated and bubbled with pure nitrogen to remove the undesirable oxygen which selectively quenches the slow component of light emission. A shiny aluminum foil reflector and a 0.63-cm-thick plastic light pipe reduced the variation in response over most of the length of the scintillator to roughly 3%, or $\frac{1}{3}$ of that with white paint and without light pipe, as determined with a narrow beam of ^{60}Co gamma rays. The greatest improvement was realized near the photocathode. These improvements apply only to our scintillator geometry, and were found to actually degrade the performance of an 8-cm-dia. spherical scintillator with flat bottom.

3. Method of absolute calibration

With the experimental and data-handling techniques outlined in sections 5 and 6, we obtained 20 pulse-height distributions for nearly monoenergetic neutrons between 0.2 and 22 MeV. Assuming that the half height of the abrupt edge near the maximum pulse height corresponds to the maximum hydrogen recoil energy, a trial function, $L_p(E)$, of proton light vs energy was constructed. Next, a preliminary series of Monte Carlo calculations was carried out at the 20 values of E_n with the experimental spread of neutron energy factored in. The calculated pulse-height distributions were convoluted with a Gaussian smearing function and integrated over the width of each pulse-height bin, so that they matched the measured pulse-height distributions. In this matching process the errors in the $L_p(E)$ function were determined, the function was corrected, and the Monte Carlo calculation was repeated with the correct $L_p(E)$. Values of $L_p(E)$ are given in table 1, with an estimated accuracy of 2% from 0.3 to 22 MeV. Values for similar functions for alpha particles and carbon-recoil ions, $L_\alpha(E)$ and $L_c(E)$, are also given in table 1. They are known much less accurately than $L_p(E)$, but their accuracy has no direct bearing on the calibrations presented here.

TABLE 1

Light output in pulse-height units. One unit is defined by 1.28-MeV ^{22}Na gamma-ray Compton edge presented in table 3. See also top of fig. 3. Estimated errors are 2% for protons from 0.3 to 20 MeV, 10% for alpha particles from 0.5 to 9 MeV, and 25% for carbon ions from 0.5 to 4 MeV.

Energy (MeV)	$L_p(E)$, protons	$L_c(E)$, carbon	$L_\alpha(E)$, alpha particles
0.1000	0.006710	0.001038	0.001640
0.1300	0.008860	0.001270	0.002090
0.1700	0.012070	0.001573	0.002720
0.2000	0.014650	0.001788	0.003200
0.2400	0.018380	0.002076	0.003860
0.3000	0.024600	0.002506	0.004900
0.3400	0.029000	0.002793	0.005640
0.4000	0.036500	0.003191	0.006750
0.4800	0.048300	0.003676	0.008300
0.6000	0.067800	0.004361	0.010800
0.7200	0.091000	0.005023	0.013500
0.8400	0.117500	0.005686	0.016560
1.000	0.156200	0.006569	0.021000
1.300	0.238500	0.008128	0.030200
1.700	0.366000	0.010157	0.044100
2.000	0.472500	0.011647	0.056200
2.400	0.625000	0.013634	0.075000
3.000	0.866000	0.016615	0.110000
3.400	1.042000	0.018713	0.136500
4.000	1.327000	0.021859	0.181500
4.800	1.718000	0.026054	0.255500
6.000	2.310000	0.032347	0.407000
7.200	2.950000	0.038750	0.607000
8.400	3.620000	0.045154	0.870000
10.00	4.550000	0.053986	1.320000
13.00	6.360000	0.071346	2.350000
17.00	8.830000	0.098808	4.030000
20.00	10.800000	0.121440	5.440000
24.00	13.500000	0.153456	7.410000
30.00	17.700000	0.206448	10.420000
34.00	20.500000	0.246192	12.440000
40.000	24.800000	0.312432	15.500000

After fitting the experimental data, the Monte Carlo calculations and Gaussian smearing were finally carried out at the mid-band energy of each "monoenergetic" neutron group and the experimental pulse-height spectra were normalized to the calculated curves in the proton-recoil plateau, the experimental data thereby being converted to absolute differential efficiency.

4. The Monte Carlo calculations and absolute checks

An accurate calculation of pulse-height distributions for neutrons up to 22 MeV incident on an organic scintillator is not possible without a complete know-

* Manufactured by Nuclear Enterprises, Ltd., Winnipeg, Canada.

TABLE 2
Computed total efficiency and total cross sections for Monte Carlo calculation and for analytic calculation.

Neutron energy (MeV)	Number of neutrons detected	Monte Carlo total efficiency	$\sigma_t(^1H)$ (b)	$\sigma_t(^{12}C)$ (b)	Analytic efficiency
0.2015	10,000	0.8727	9.523	4.260	0.8728
0.3220	10,000	0.8212	7.719	3.857	0.8292
0.4265	10,000	0.7974	6.712	3.583	0.7958
0.6170	10,000	0.7353	5.532	3.174	0.7436
0.9035	10,000	0.6770	4.515	2.720	0.6816
1.205	20,000	0.6280	3.902	2.345	0.6309
1.613	20,000	0.5692	3.287	1.965	0.5706
2.234	40,000	0.5040	2.737	1.606	0.5058
3.329	40,000	0.4571	2.183	1.760	0.4690
4.236	40,000	0.4485	1.827	1.943	0.4502
4.919	40,000	0.3688	1.646	1.198	0.3704
6.017	40,000	0.3343	1.422	1.094	0.3358
7.038	40,000	0.2999	1.246	1.023	0.3082
8.029	40,000	0.3358	1.137	1.466	0.3380
10.00	40,000	0.2802	0.940	1.140	0.2825
11.98	40,000	0.2744	0.801	1.259	0.2773
14.01	40,000	0.2725	0.693	1.360	0.2741
16.06	40,000	0.2664	0.605	1.431	0.2703
17.81	40,000	0.2628	0.541	1.448	0.2640
19.91	40,000	0.2569	0.483	1.450	0.2566
21.81	40,000	0.2482	0.442	1.445	0.2508

ledge of the various neutron reactions with carbon. This includes light production functions and the correct "smearing" for alpha particles and carbon recoils, the cross sections, branching ratios to various levels of the excited residual nucleus, and angular distributions of the reaction products. Since, however, these reactions produce pulses much smaller than the largest proton-recoil pulses, use of the correct nonelastic cross section (the sum of all the cross sections for reactions which deplete the proton-recoil plateau) with the Monte Carlo code[1]) accurately predicts the absolute differential efficiency for the proton-recoil plateau. The absolute differential efficiency at neutron energy E_n as applied to the calibrations presented below is defined as the curve of counts per unit pulse height, normalized to 1 neutron incident on the cross-sectional area of the scintillator.

Each Monte Carlo calculation was checked with an analytic calculation in which the total neutron-removal probability $[1-\exp(-\Sigma_t T)]$ was averaged over all pathlengths T through the scintillator. The calculated Monte Carlo total (zero bias) efficiencies are compared with the analytic calculations in table 2. The total hydrogen and carbon cross sections upon which these efficiencies depend are also given. The variation between the Monte Carlo and the analytic results is due to the finite number of histories in the Monte Carlo calculation.

The calculations performed for the 0.2- to 22-MeV calibrations reported here took into account proton-recoil leakage from the scintillator and nonisotropy (in the center-of-mass coordinates) of the recoil-proton angular distribution above 12 MeV. For these calculations the density of NE-213 was taken as 0.867 g/cm^3 and the composition as $CH_{1.21}$ as given in the manufacturer's specifications. The hydrogen density is known to better than 1%, and the hydrogen cross section[4]) to 1% from 0.2 to 22 MeV.

The estimates of the various cross sections for neutron interactions with ^{12}C and the method of carrying out the Monte Carlo calculations are described elsewhere[1]). The accuracy of these calculations in the proton-recoil plateau region is indicated by some absolute experimental calibrations presented in[5]).

The results of the absolute measurements were compared[5]) with Monte Carlo calculations for the same scintillators and the same neutron energies, and the agreement was better than 5% in the proton-recoil plateau when the proton-recoil edges were carefully matched. These early Monte Carlo calculations assumed isotropic recoil-proton scattering above 12 MeV. The calculations have recently been repeated with the inclusion of the non-isotropic angular distribution[6]) at 14 MeV, and the inferred agreement in the upper end of the proton-recoil plateau was improved to about $2\frac{1}{2}$%.

Some additional associated-particle runs were made that were relative rather than absolute[7]). They were useful in determining the pulse-shape discriminator losses at low pulse heights, as described below, and for obtaining points on the L_e and L_α light production curves given in table 1.

An additional associated-particle run made with a 5-cm NE-211 scintillator and 14.4-MeV neutrons gave the same result as with NE-213 over a 700:1 pulse-height range, with each normalized to the same ^{60}Co and ^{113}Sn gamma-ray pulse-height spectrum. This demonstrated that the responses of the two scintillators are identical to within an estimated 3% matching accuracy for neutrons when the light pulses are integrated by a 1.5-μsec double-delay-line amplifier. The results of the two high-gain runs are shown in fig. 1, along with the ^{113}Sn calibration spectrum.

5. Experimental arrangements for 0.2- to 22-MeV calibration

The Oak Ridge National Laboratory 5-MV Van de Graaff generator was used in a pulsed mode to provide

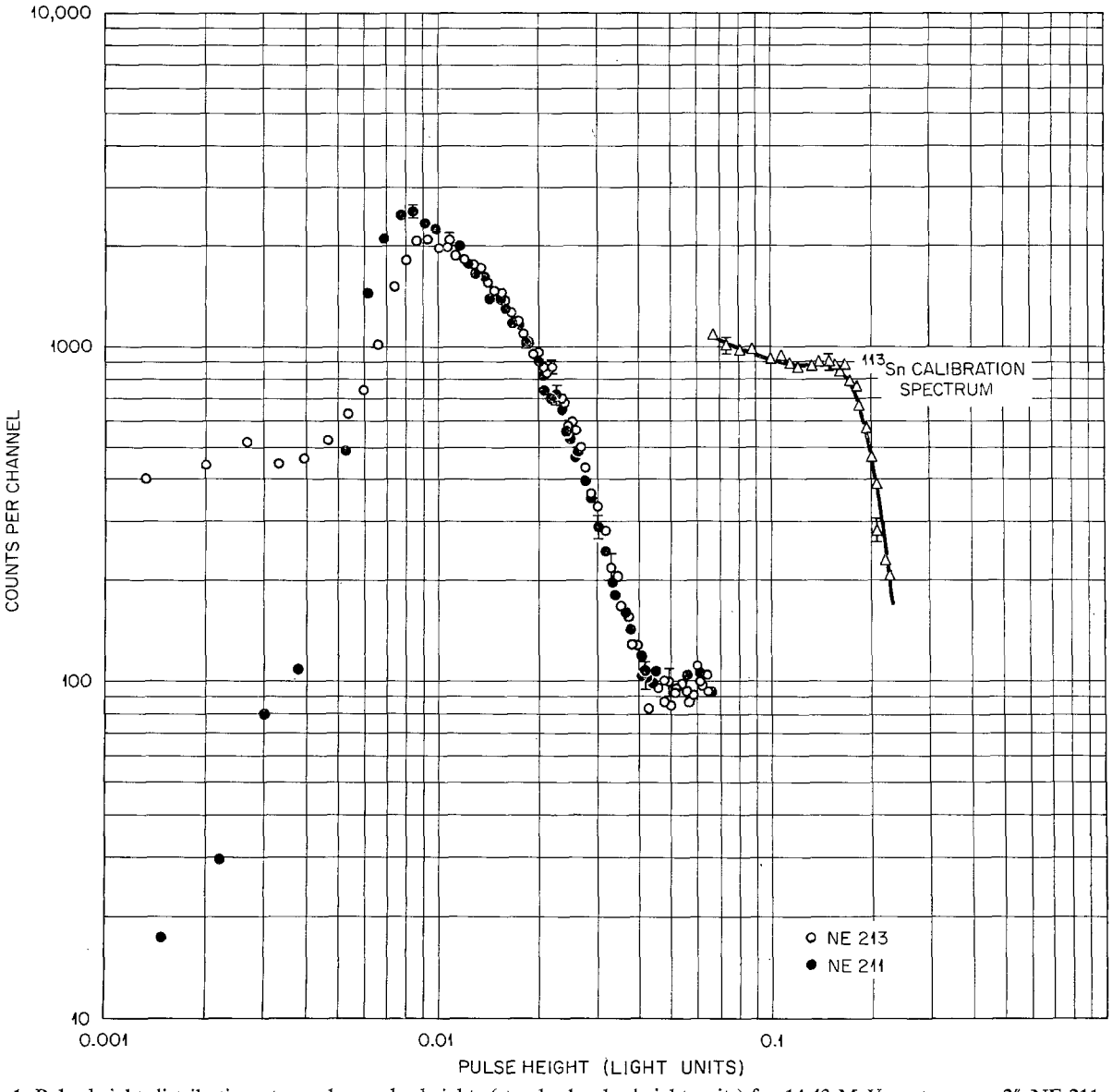

Fig. 1. Pulse-height distribution at very low pulse heights (standard pulse-height units) for 14.43-MeV neutrons on 2″ NE-211 and NE-213 scintillators obtained with associated-particle technique. This indicates that the two scintillators are equal in response to neutrons. The carbon-recoil edge appears below 0.04 unit of pulse height. Below 0.01 unit, instrument bias effects are evident.

about 2-nsec bursts of protons or deuterons. Flight paths of 1–5 m were used. The $T(p,n)^3He$, $D(d,n)^3He$, and $T(d,n)^4He$ reactions were utilized to provide neutrons in the respective energy ranges of 0.2 to 4.22, 4.92 to 8.03 and 12.0 to 21.8 MeV. The targets for the three ranges consisted, respectively, of a 0.40-mg/cm^2-thick ^{3}H-Zr target on platinum backing, producing a neutron energy spread ΔE_n of less than 30 keV; a deuterium gas target of about 2 atm pressure and 0.65 cm thickness ($\Delta E_n < 70$ keV) with a 0.00025-cm-thick Havar* window; and a 4.3-mg/cm^2-thick T-Er target mounted on Cu($\Delta E_n \simeq 0.3$ MeV). We used a beam-energy calibration performed at 4.642 MeV by Kernell and Robinson of ORNL†, which was estimated to be accurate to better than 10 keV. Extrapolation to other energies was accomplished with the aid of fig. 1 of ref. [6]).

In each case a horizontal beam of neutrons was in-

* Precision Metals Division, Hamilton Watch Co., Lancaster, Pennsylvania.

† We are indebted to R. L. Robinson for making this calibration available.

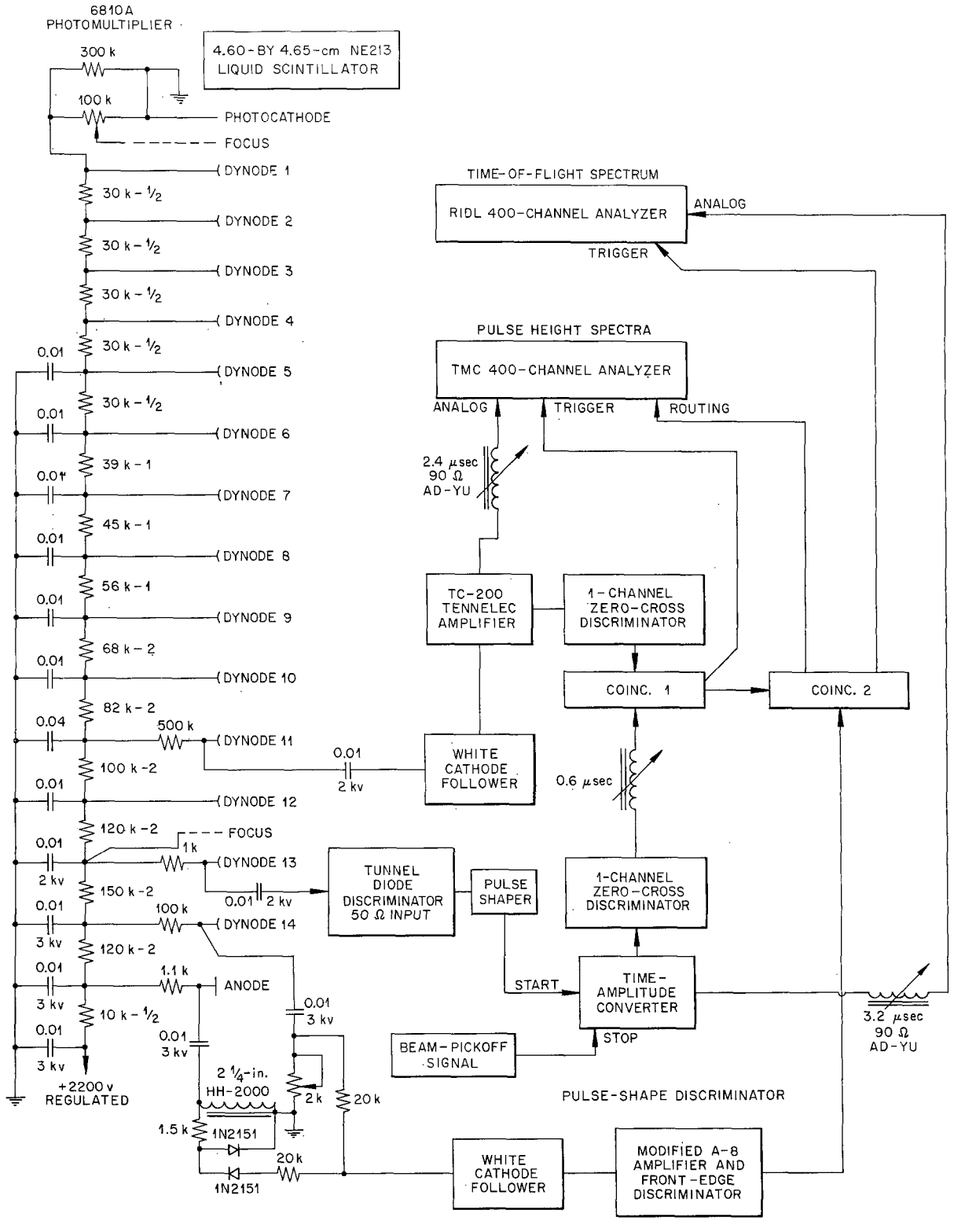

Fig. 2. Block diagram for 0.2- to 22-MeV calibrations, including details of photomultiplier tube base circuit.

cident on the curved surface (perpendicular to the axis) of the 4.60- by 4.65-cm-dia. NE-213 scintillator. The scintillator was mounted on a 0.63-cm-thick, 5-cm-dia. Plexiglas light pipe, which was mounted on an RCA 6810A photomultiplier tube selected by the manufacturer for about 100 μA/lumen photocathode efficiency and an anode sensitivity of 1800 A/lumen (manufacturer's standard testing conditions) with light from a tungsten lamp at 2870° K color temperature. Scattering by the 1.5-mm-thick glass walls of the scintillator container and by other surrounding material introduced an error which was small, as estimated by a Monte Carlo calculation, compared with the overall error.

In fig. 2 is shown the circuit diagram for the photomultiplier tube base with signals taken from dynode 11 for a linear signal, from dynode 13 for a fast timing signal, and from dynode 14 and the anode for two signals for the pulse-shape discriminator circuit. A neutron of the proper energy arrives at the scintillator at a time that causes the output or the time-to-amplitude converter to fall in the window of a single-cannel discriminator. A pulse from this discriminator and one from the linear amplifier discriminator activate coincidence 1, which triggers a Technical Measurement Corporation pulse-height analyzer. Pulses from coincidence 1 activate coincidence 2 when the pulse-shape discriminator identifies the pulse as a neutron event, which causes the pulse to be stored in the second half of the analyzer's memory. A gamma-ray pulse, or any other pulse which activates coincidence 1 but not coincidence 2, is stored in the first half of the analyzer. At neutron energies below 3 MeV, very few gamma rays are produced with the ^{3}H(p,n)^{3}He reactions, and pulses stored in the first half are all neutron pulses rejected by the discriminator. When these data were added to the data in the second half of the analyzer, the correct pulse-height spectrum was obtained, for $E_n < 3$ MeV, without the use of the correction factor presented in the next section; actually, these data provided an independent check on the correction factor.

An important point is that all leads in the photomultiplier tube base were kept short and near the ground bus to reduce pickup at dynode 11 of the much larger pulses at dynodes 13 and 14 and the anode. Dynode 11 was

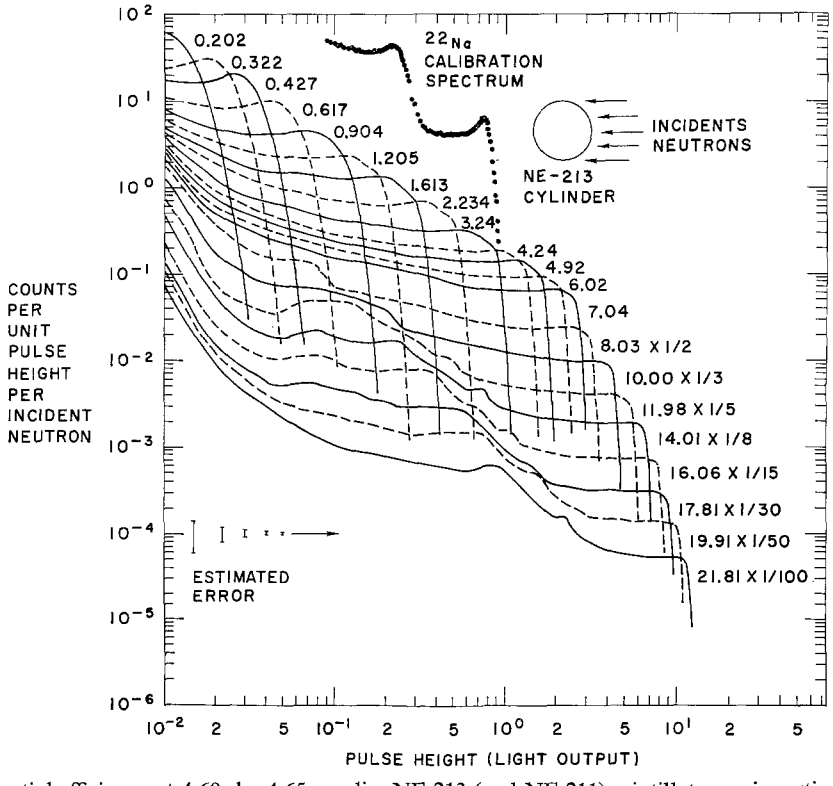

Fig. 3. Absolute differential efficiency at 4.60- by 4.65-cm-dia. NE-213 (and NE-211) scintillator, axis vertical, in horizontal, plane-wave neutron field, normalized to 1 neutron incident on cross sectional area ($h \times 2r$). The area of a given curve above a bias level thus represents the average efficiency for producing pulses above this bias. The 10-MeV response is an interpolation between the 8- and 12-MeV responses (see text). Use tables for good accuracy. The pulse-height scale is defined by the spectrum shown for incident gamma rays from a ^{22}Na source.

TABLE 3
Pulse-height distribution of Compton edge of 1.28-MeV ^{22}Na gamma-ray line which defines one light unit for the 4.60- by 4.65-cm-dia. NE-213 (and NE-211) scintillator, at the pulse-height resolution implied here. For use with a system having worse resolution, the data here should be smeared to match the system's resolution.

Average pulse height	Counts per interval	Average pulse height	Counts per interval
0.740	2321	0.870	2106
0.750	2413	0.880	1815
0.760	2545	0.890	1551
0.770	2587	0.900	1268
0.780	2664	0.910	1008
0.790	2765	0.920	838
0.800	2839	0.930	705
0.810	2868	0.940	515
0.820	2886	0.950	378
0.830	2793	0.960	269
0.840	2795	0.970	221
0.850	2600	0.980	173
0.860	2400	0.990	79

chosen for the linear output because it was the highest dynode number from which a linear signal could be obtained without saturation under the operating conditions of the photomultiplier tube. With these techniques good data reproducibility was obtained for four 6180A photomultiplier tubes. Their photocathode sensitivities ranged from 95 to 120 μA/lumen.

6. Counting technique for 0.2- to 22-MeV calibrations

Gain standardization has been found to be one of the most troublesome problems in reproducing the experimental measurements and communicating the calibration procedures to other laboratories. The best approach is to ensure that the ^{22}Na pulse-height spectrum, measured at the time of a neutron-spectroscopy experiment, has the same position on the pulse-height scale as the calibration shown at the top of fig. 3. Because of probable plotting inaccuracies, a similar calibration is given in table 3 for making detailed graphical comparisons. These data precisely define "one light unit" for the calibrations presented here. This unit is approximately equal to the light produced by 1.25-MeV electrons according to the prescription of Flynn et al.[9]), or 13% above the 1.28-MeV Compton edge half-height for our system.

In order to apply the gain calibration of table 3 to a system utilizing the same size scintillator but with poorer energy resolution, the Compton edge of the 1.28-MeV ^{22}Na would have to be smeared correctly to match the poor-resolution spectrum.

All measurements were made with the TC-200 amplifier time constants set at 0.8, 0.8 and 0.8 μsec for the first and second differentiation and for the integration. A precision pulser, adjusted to match the neutron pulse-shape output from the preamplifier, was used to optimize the system linearity and zero-channel setting.

Another important calibration consisted of a measurement of the pulse-height distribution due to neutrons from a ^{241}Am-Be source. The source was surrounded with a 0.25-cm-thick lead sheet to reduce the high count rate from 60-keV gammas. A typical pulse-height distribution of this type is shown as the lower curve in fig. 4. The upper curve is the true Am-Be pulse-height spectrum obtained by correcting the lower curve for pulse-shape discriminator losses at low pulse heights. The pulse-shape discriminator loss as a function of pulse height was obtained from two associated-particle coincidence measurements of 2.66-MeV neutrons, one with and one without the use of the neutron-gamma pulse-shape discriminator. The two differ only by the losses of the pulse-shape discriminator since essentially no gamma-ray pulses occurred in coincidence with the detected ^{3}He ions.

Before each measurement of a response function, a time-of-flight spectrum was obtained on the RIDL analyzer shown in the block diagram in fig. 2. This spectrum was used to set the amplitude window on the single-channel analyzer following the time-to-amplitude converter to accept only the peak in the time spectrum corresponding to monoenergetic neutrons. The time window had to be set to about a 15-nsec width because of the walk in the fast-timing tunnel-diode discriminator. In addition, the discriminator level had to be set low to prevent the pulse-height distribution from being distorted because of some pulses being missed in the wings of the peak in the spectrum. The distance between the target and the detector was varied between 1 and 5 m to optimize the count rate and the separation of the monoenergetic neutrons from spurious neutrons arising from reactions with the target foils. Using this flight-time selection, the amplitude spectrum for monoenergetic neutrons was measured at from one to four different gain settings: one gain was used at low energies and four gains were used at 20 and 22 MeV, where a 1000:1 range in pulse heights had to be measured. For each gain setting, the "gamma" pulses were stored in the first half of the TMC-400 channel analyzer and the "neutron" pulses in the second half. A background measurement was also made in each case by using a 50-cm-long iron shadow shield located about half-way between the neutron source and scintillator. This measurement was used to correct for

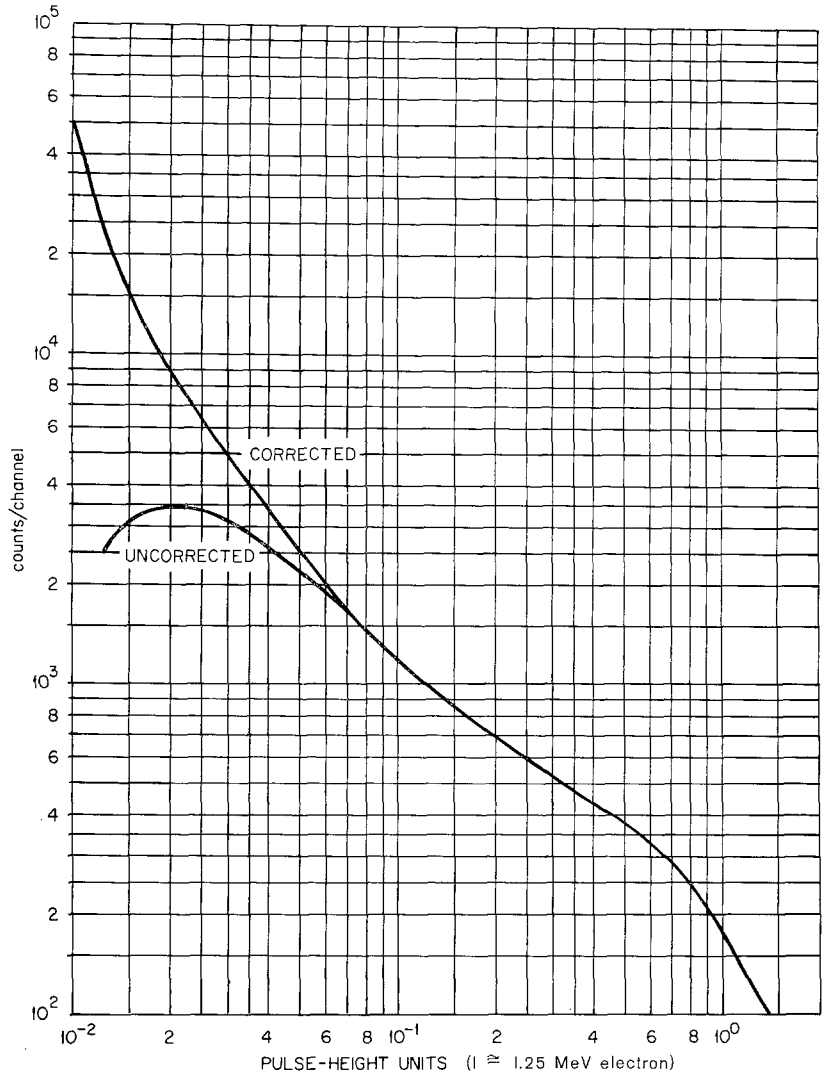

Fig. 4. Pulse-height distribution for small ^{241}Am-Be neutron source in 0.25-cm-thick lead shield. Lower curve shows losses due to pulse-shape discriminator. Upper curve shows corrected pulse-shape distribution, with corrections obtained from associated-particle measurements made at 2.66 MeV both with and without pulse-shape discriminator.

neutrons produced on the sides of the beam pipe or for neutrons scattered into the scintillator by the photomultiplier and other materials nearby. Backgrounds were typically 5 to 10% and were not much different in shape from the total spectrum. During all runs a current integrator that gave a measure of total charge incident on the target was used to help achieve proper foreground-background normalization and gain-to-gain normalization for multiple gain runs at each neutron energy.

7. Data analysis and results

All data were normalized to a standard gain and corrected for zero-drift, for a small analyzer nonlinearity, for background counts, and for pulse-shape discriminator losses. The multiple gain runs were combined by normalizing one to another in a predetermined overlap region, the data were grouped to a minimum of two bins per resolution width, and the results were plotted on a scale similar to that of fig. 3. The flat region, the recoil-proton plateau, of each measured pulse-height distribution was then normalized to the corresponding region of a Monte Carlo-calculated pulse-height distribution for the same neutron energy. This normalization is equivalent to equating the area of the experimental curve that lies above the lowest

TABLE 4

Absolute differential efficiency versus pulse height (table 3) of a 4.60- by 4.65-cm-dia. NE-213 or NE-211 scintillator irradiated on curved side by plane parallel beam of monoenergetic neutrons perpendicular to scintillator axis. The lower edge of each pulse height bin L is given. The bin widths are all fractionally equal, or $\Delta L/L \cong 4.42\%$.

Pulse height	Absolute differential efficiencies for neutron energies of										
	0.201 MeV	0.322 MeV	0.427 MeV	0.617 MeV	0.904 MeV	1.205 MeV	1.613 MeV	2.233 MeV	3.238 MeV	4.236 MeV	4.919 MeV
0.01540	30.59834	28.45300	16.39100	9.39167	5.81642	4.34592	3.33900	2.67633	2.10111	1.39750	1.25127
0.01608	26.14258	29.00800	16.46500	9.23833	5.63896	4.18458	3.21300	2.55233	1.96599	1.32383	1.14623
0.01679	20.90256	30.02744	16.54825	9.10417	5.46152	4.04342	3.08280	2.42213	1.81249	1.21550	1.05262
0.01753	17.08856	30.62817	16.58525	8.91250	5.34322	3.90225	2.96520	2.29813	1.69985	1.15050	0.99325
0.01830	12.90451	31.06902	16.63150	8.70167	5.22492	3.78125	2.83920	2.17000	1.56986	1.07813	0.91105
0.01912	10.06327	31.10483	16.72400	8.54833	5.10662	3.66025	2.73000	2.08320	1.47378	1.01313	0.86082
0.01995	7.14930	30.66677	17.05700	8.43333	4.94888	3.51908	2.61240	1.96747	1.36316	0.95333	0.79917
0.02084	5.30202	29.88533	17.35300	8.35667	4.87002	3.43842	2.51160	1.89307	1.28219	0.91433	0.75350
0.02175	3.53007	28.34000	18.01900	8.27042	4.72214	3.34767	2.39400	1.80833	1.19037	0.86667	0.70327
0.02272	2.48217	26.65870	18.61100	8.23208	4.64327	3.26700	2.30160	1.75047	1.12436	0.83200	0.66673
0.02371	1.54267	24.06309	19.19177	8.18417	4.54426	3.15608	2.22180	1.68020	1.05094	0.79733	0.62221
0.02477	1.02527	21.66855	19.62764	8.14583	4.50306	3.07542	2.13780	1.61407	0.99920	0.76700	0.60166
0.02585	0.59231	18.42651	19.98378	8.12667	4.40667	2.97862	2.03616	1.54587	0.94274	0.73017	0.57768
0.02700	0.37083	15.75497	20.06649	8.20333	4.28837	2.91812	1.93536	1.47973	0.90366	0.70850	0.55942
0.02818	0.19821	12.49531	19.85125	8.35667	4.20951	2.84350	1.87740	1.41773	0.86167	0.67600	0.54115
0.02943	0.11646	10.06412	19.38919	8.37958	4.13064	2.76283	1.82700	1.37640	0.83297	0.65000	0.52745
0.03073	0.05730	7.37153	18.42450	8.51136	4.07149	2.71242	1.76694	1.32887	0.80229	0.61317	0.50918
0.03208	0.03147	5.55019	17.34760	8.66836	4.03994	2.67208	1.72746	1.28753	0.78124	0.59583	0.49092
0.03350	0.01417	3.71865	15.66188	8.88852	4.04191	2.61158	1.66950	1.24207	0.75834	0.56767	0.47265
0.03497	0.00724	2.59803	14.09449	9.07905	4.04980	2.55558	1.64430	1.20073	0.74210	0.55033	0.45895
0.03652	0.00297	1.57746	11.96416	9.32250	4.05966	2.51331	1.61994	1.15940	0.72358	0.52867	0.44068
0.03813	0.00140	1.01535	10.20608	9.50786	4.06375	2.48189	1.59558	1.13047	0.70974	0.51350	0.42698
0.03981	0.00052	0.55354	8.06193	9.70246	4.05642	2.44734	1.55526	1.09120	0.69322	0.49833	0.41328
0.04157	0.00022	0.32596	6.46553	9.80817	4.05352	2.42348	1.53342	1.07053	0.68046	0.48750	0.39958
0.04340	0.00007	0.15807	4.70285	9.84906	4.05729	2.39796	1.52124	1.04367	0.66508	0.47017	0.38360
0.04532	0.00003	0.08457	3.51562	9.79148	4.06711	2.38039	1.50864	1.02300	0.65334	0.45283	0.37218
0.04732	0.00001	0.03614	2.32859	9.58954	4.08919	2.36087	1.49478	0.98787	0.63963	0.44092	0.36077
0.04941		0.01745	1.60792	9.31817	4.11538	2.34633	1.48302	0.96307	0.62962	0.43442	0.35391
0.05158		0.00651	0.95816	8.84100	4.15911	2.32856	1.46958	0.94447	0.61717	0.42250	0.34365
0.05387		0.00282	0.60518	8.35239	4.20264	2.31436	1.45950	0.92793	0.60587	0.40950	0.33451
0.05623		0.00091	0.32021	7.61658	4.26663	2.29691	1.44942	0.91170	0.59167	0.39433	0.32355
0.05873		0.00035	0.18307	6.93650	4.32411	2.28381	1.44186	0.90233	0.58220	0.38567	0.31670
0.06131		0.00010	0.08480	5.99130	4.40044	2.26962	1.42800	0.88858	0.56445	0.37483	0.30619
0.06400		0.00003	0.04341	5.17998	4.40306	2.26075	1.41960	0.87553	0.54788	0.36617	0.29934
0.06683		0.00001	0.01735	4.14023	4.40470	2.25345	1.40910	0.85630	0.53132	0.35533	0.29341
0.06979			0.00787	3.32650	4.40470	2.25086	1.39482	0.83864	0.52422	0.34424	0.28656
0.07286			0.00267	2.39075	4.38499	2.25177	1.38066	0.81430	0.51238	0.33337	0.27971
0.07609			0.00106	1.74348	4.35738	2.25580	1.36479	0.79382	0.49818	0.32568	0.27423
0.07943			0.00030	1.09407	4.30809	2.26517	1.34431	0.76858	0.48398	0.31611	0.26761
0.08295			0.00011	0.70810	4.26866	2.27639	1.32801	0.74989	0.47452	0.30881	0.26030

0.08660	0.00002	0.37750	4.13832	2.29565	1.30804	0.72994	0.46268	0.30052	0.25322
0.09043		0.21256	3.94568	2.31541	1.29227	0.71728	0.45322	0.29474	0.24820
0.09441		0.09391	3.67992	2.34486	1.27260	0.70562	0.43783	0.28854	0.24203
0.09858		0.04521	3.45556	2.37070	1.25694	0.69913	0.42837	0.28412	0.23609
0.10292		0.01618	3.16304	2.40201	1.25706	0.69342	0.42127	0.27877	0.22948
0.10748		0.00656	2.92645	2.42271	1.25538	0.68987	0.41653	0.27428	0.22674
0.11220		0.00186	2.59274	2.43745	1.25328	0.68542	0.40352	0.27278	0.22285
0.11717		0.00063	2.32853	2.43633	1.25160	0.68115	0.40020	0.26975	0.22103
0.12232		0.00014	1.95589	2.41339	1.24950	0.67424	0.39689	0.26498	0.21829
0.12773		0.00004	1.61677	2.37487	1.24782	0.66739	0.39310	0.26108	0.21463
0.13335		0.00001	1.11399	2.30028	1.23900	0.65756	0.38932	0.25675	0.21029
0.13925			0.81824	2.22116	1.23060	0.64919	0.38600	0.25415	0.20709
0.14538			0.43499	2.05700	1.25789	0.63699	0.38222	0.24878	0.20276
0.15181			0.23112	1.93600	1.28000	0.62723	0.37512	0.24583	0.19865
0.15849			0.10225	1.79080	1.30805	0.62207	0.36660	0.24150	0.19385
0.16550			0.04827	1.71013	1.30475	0.61793	0.36328	0.23664	0.19066
0.17278			0.01628	1.61333	1.29360	0.60863	0.35737	0.23487	0.18723
0.18043			0.00612	1.52057	1.28940	0.60533	0.35358	0.23053	0.18449
0.18836			0.00151	1.32293	1.28415	0.60739	0.35098	0.22533	0.18038
0.19670			0.00044	1.16160	1.27995	0.60905	0.34908	0.22187	0.17901
0.20535			0.00007	0.85103	1.27470	0.61111	0.34317	0.21927	0.17490
0.21444			0.00002	0.59693	1.25279	0.61277	0.34033	0.21753	0.17308
0.22387				0.32098	1.18904	0.61483	0.33820	0.21277	0.16942
0.23378				0.17654	1.13313	0.61649	0.33252	0.21017	0.16760
0.24406				0.07090	1.05840	0.61855	0.32542	0.20843	0.16554
0.25486				0.02950	0.99120	0.62021	0.32068	0.20800	0.16280
0.26607				0.00794	0.90720	0.62103	0.31548	0.20800	0.15983
0.27784				0.00239	0.84420	0.62145	0.31358	0.20800	0.15709
0.29007				0.00041	0.78540	0.62827	0.31216	0.20761	0.15298
0.30290				0.00009	0.72240	0.63653	0.31074	0.20713	0.15162
0.31623				0.00001	0.56652	0.64687	0.30838	0.20453	0.14978
0.33022					0.40942	0.65513	0.30648	0.20107	0.14888
0.34475					0.22978	0.66133	0.30412	0.19673	0.14773
0.35999					0.12299	0.65720	0.30222	0.19327	0.14682
0.37584					0.04465	0.64480	0.29986	0.18893	0.14544
0.39246					0.01632	0.60967	0.29796	0.18547	0.14362
0.40973					0.00345	0.56627	0.29654	0.18352	0.14134
0.42786					0.00082	0.53320	0.29844	0.18352	0.13951
0.44668					0.00010	0.48546	0.30080	0.18191	0.13746
0.46644					0.00001	0.47033	0.30270	0.18148	0.13609
0.48697						0.44103	0.30506	0.18027	0.13533
0.50851						0.40548	0.30696	0.17853	0.13455
0.53088						0.32550	0.30932	0.17377	0.13302
0.55437						0.21927	0.31122	0.17117	0.13181
0.57876						0.09718	0.30767	0.17182	0.13117
0.60436						0.04133	0.30293	0.17182	0.13197
0.63096						0.00980	0.29583	0.17160	0.13404

(continued on p. 18)

TABLE 4 *(continued)*

Absolute differential efficiencies for neutron energies of

Pulse height	0.201 MeV	0.322 MeV	0.427 MeV	0.617 MeV	0.904 MeV	1.205 MeV	1.613 MeV	2.233 MeV	3.238 MeV	4.236 MeV	4.919 MeV
0.65886								0.00233	0.28353	0.17030	0.13477
0.68786								0.00023	0.26909	0.16976	0.13299
0.71828								0.00003	0.26152	0.17019	0.13055
0.74989									0.24377	0.17160	0.12871
0.78306									0.23099	0.17203	0.12836
0.81752									0.22176	0.17290	0.12802
0.85368									0.20898	0.17333	0.12756
0.89125									0.18697	0.17377	0.12788
0.93067									0.14910	0.17507	0.12928
0.97163									0.07147	0.17420	0.13144
1.01460									0.02989	0.17030	0.13239
1.05925									0.00617	0.16250	0.13231
1.10610									0.00118	0.15600	0.13266
1.15478									0.00007	0.14733	0.13380
1.20586										0.14083	0.13335
1.25893										0.12913	0.13106
1.31460										0.11700	0.12787
1.37246										0.09187	0.11919
1.43316										0.05503	0.11326
1.49624										0.01967	0.10549
1.56241										0.00520	0.10092
1.63117										0.00023	0.08996
1.70331										0.00002	0.07096
1.77828											0.03212
1.85693											0.01016
1.93865											0.00109
2.02439											0.00011

Absolute differential efficiencies for neutron energies of

Pulse height	6.017 MeV	7.037 MeV	8.029 MeV	10.000 MeV	11.980 MeV	14.007 MeV	16.055 MeV	17.805 MeV	19.907 MeV	21.809 MeV
0.01540	0.99147	0.87165	1.37280	1.21250	1.08900	0.96900	0.82820	1.03192	1.34000	1.99500
0.01608	0.91520	0.79715	1.25400	1.06700	0.90420	0.86360	0.73562	0.92264	1.17333	1.77833
0.01679	0.83893	0.71520	1.12200	0.91342	0.71940	0.75990	0.64303	0.78494	0.99333	1.55833
0.01753	0.79127	0.66057	1.02960	0.79702	0.62370	0.68850	0.57907	0.69697	0.89667	1.39167
0.01830	0.73168	0.61090	0.92840	0.70002	0.52140	0.60010	0.50837	0.59885	0.79833	1.20333
0.01912	0.68878	0.58110	0.84480	0.62242	0.46860	0.54230	0.45450	0.53964	0.71833	1.07000
0.01995	0.64588	0.53888	0.77220	0.55613	0.41415	0.48280	0.40400	0.48805	0.64167	0.95833

0.02084	0.61252	0.51405	0.72820	0.51410	0.37950	0.43520	0.37202	0.45185	0.59167	0.87500
0.02175	0.57200	0.48300	0.67430	0.46156	0.33825	0.37440	0.34004	0.41446	0.53500	0.79833
0.02272	0.54578	0.46066	0.62370	0.43084	0.31515	0.34680	0.32152	0.38740	0.49500	0.73500
0.02371	0.51718	0.43458	0.57530	0.40417	0.29288	0.31450	0.29626	0.36202	0.44833	0.66167
0.02477	0.49812	0.41720	0.54010	0.38638	0.27638	0.28900	0.27775	0.33664	0.42167	0.61167
0.02585	0.47547	0.39981	0.50820	0.36779	0.26070	0.25925	0.25586	0.30788	0.39250	0.56000
0.02700	0.45879	0.38243	0.48180	0.34354	0.25410	0.24395	0.24072	0.29266	0.37083	0.52333
0.02818	0.43520	0.36629	0.45100	0.33061	0.24090	0.22525	0.22136	0.27151	0.34500	0.47750
0.02943	0.42090	0.35387	0.42900	0.31606	0.23430	0.21165	0.21126	0.25459	0.32167	0.45083
0.03073	0.40278	0.33525	0.40040	0.29827	0.22308	0.19890	0.19880	0.23768	0.29583	0.41917
0.03208	0.38848	0.32283	0.37620	0.28695	0.21483	0.19040	0.19207	0.22584	0.28083	0.39583
0.03350	0.37537	0.30669	0.35640	0.26917	0.20691	0.18156	0.18584	0.21366	0.26167	0.37333
0.03497	0.36346	0.29924	0.34320	0.25947	0.20031	0.17476	0.18113	0.20385	0.24833	0.35500
0.03652	0.35154	0.28509	0.33110	0.24735	0.19371	0.16813	0.17372	0.19150	0.23167	0.33167
0.03813	0.34201	0.27565	0.32318	0.23927	0.18909	0.16269	0.16733	0.18270	0.21833	0.31667
0.03981	0.33009	0.26696	0.31614	0.22956	0.18398	0.15504	0.15908	0.17255	0.20667	0.29417
0.04157	0.32294	0.25951	0.30998	0.22633	0.18002	0.15062	0.15436	0.16747	0.19700	0.27917
0.04340	0.31579	0.25106	0.30250	0.22229	0.17523	0.14450	0.15234	0.16274	0.18433	0.26167
0.04532	0.30625	0.24560	0.29810	0.21970	0.17259	0.14144	0.15167	0.15834	0.17600	0.24833
0.04732	0.29792	0.23939	0.29282	0.21728	0.17490	0.14110	0.15218	0.15546	0.16700	0.23250
0.04941	0.29076	0.23592	0.29062	0.21534	0.17919	0.14144	0.15352	0.15546	0.16267	0.22083
0.05158	0.28243	0.22747	0.28798	0.21308	0.18678	0.14195	0.15605	0.15733	0.15700	0.21000
0.05387	0.27385	0.22400	0.28798	0.21178	0.19338	0.14297	0.15908	0.15902	0.15233	0.20033
0.05623	0.26598	0.21729	0.28886	0.21017	0.20543	0.14773	0.16126	0.16054	0.14667	0.18867
0.05873	0.26026	0.20984	0.28490	0.20887	0.21368	0.15215	0.16396	0.16121	0.14133	0.17933
0.06131	0.25407	0.20388	0.28094	0.20726	0.22440	0.15521	0.16632	0.16206	0.13700	0.16800
0.06402	0.24596	0.19991	0.27786	0.20596	0.22935	0.15725	0.16699	0.16240	0.13367	0.16000
0.06683	0.23976	0.19444	0.27280	0.20435	0.23595	0.16065	0.16783	0.16240	0.13067	0.14967
0.06979	0.23595	0.18997	0.26840	0.20305	0.23826	0.16405	0.16850	0.16240	0.12933	0.14367
0.07286	0.22975	0.18451	0.26312	0.20176	0.23991	0.16745	0.16732	0.16172	0.12767	0.13700
0.07609	0.22403	0.18004	0.25520	0.19982	0.24123	0.16983	0.16598	0.16071	0.12600	0.13222
0.07943	0.21879	0.17557	0.23936	0.19739	0.24090	0.17272	0.16429	0.15851	0.12333	0.12700
0.08295	0.21354	0.16961	0.21560	0.19545	0.24024	0.17204	0.16295	0.15445	0.12067	0.12300
0.08660	0.20663	0.16315	0.19184	0.19335	0.23753	0.16677	0.16110	0.15039	0.11767	0.11700
0.09043	0.20282	0.16067	0.17732	0.19012	0.23727	0.16099	0.15874	0.14667	0.11633	0.11300
0.09441	0.19877	0.15570	0.15994	0.18527	0.23694	0.15504	0.15319	0.14159	0.11467	0.10733
0.09858	0.19686	0.15272	0.14674	0.18268	0.23668	0.15062	0.14813	0.13990	0.11267	0.10467
0.10292	0.19114	0.14999	0.13596	0.17864	0.23634	0.14399	0.13989	0.13770	0.10917	0.10000
0.10748	0.18638	0.14801	0.13156	0.17605	0.23608	0.14093	0.13383	0.13500	0.10650	0.09700
0.11220	0.18232	0.14627	0.12870	0.17363	0.23575	0.13600	0.12759	0.13313	0.10383	0.09583
0.11717	0.17898	0.14627	0.12606	0.16910	0.23529	0.13328	0.12322	0.13212	0.10117	0.09483
0.12232	0.17398	0.14354	0.12364	0.16425	0.22853	0.13022	0.11834	0.12941	0.09867	0.09208
0.12773	0.17112	0.14155	0.12188	0.16069	0.22028	0.12886	0.11531	0.12671	0.09733	0.09042
0.13335	0.16731	0.13932	0.11968	0.15487	0.21120	0.12682	0.11161	0.12282	0.09567	0.08817
0.13925	0.16445	0.13634	0.11748	0.14873	0.20295	0.12580	0.10952	0.11977	0.09433	0.08717
0.14538	0.15968	0.13360	0.11506	0.14275	0.18975	0.12410	0.10935	0.11554	0.09267	0.08583
0.15181	0.15683	0.13162	0.11330	0.13920	0.17919	0.12308	0.10921	0.11080	0.09133	0.08517

(continued on p. 20)

TABLE 4 *(continued)*

Pulse height	Absolute differential efficiencies for neutron energies of 6.017 MeV	7.037 MeV	8.029 MeV	10.000 MeV	11.980 MeV	14.007 MeV	16.055 MeV	17.805 MeV	19.907 MeV	21.809 MeV
0.15849	0.15372	0.12913	0.11000	0.13515	0.16681	0.12271	0.10901	0.10675	0.08950	0.08433
0.16550	0.15086	0.12715	0.10736	0.13289	0.15791	0.12247	0.10875	0.10303	0.08740	0.08333
0.17278	0.14595	0.12566	0.10516	0.12675	0.14817	0.12172	0.10895	0.10116	0.08500	0.08083
0.18043	0.14405	0.12417	0.10384	0.12319	0.14190	0.12342	0.10921	0.09981	0.08267	0.07883
0.18836	0.14162	0.12168	0.10252	0.11914	0.13447	0.12529	0.10955	0.09862	0.08000	0.07767
0.19670	0.13924	0.11970	0.10120	0.11526	0.12853	0.12665	0 10982	0.09727	0.07833	0.07633
0.20535	0.13775	0.11795	0.09944	0.10928	0.12094	0.12835	0.11019	0.09456	0.07667	0.07483
0.21444	0.13633	0.11597	0.09856	0.10250	0.11633	0.12971	0.11060	0.09118	0.07533	0.07417
0.22387	0.13394	0.11349	0.09658	0.09328	0.11171	0.12886	0.11117	0.08746	0.07367	0.07208
0.23378	0.13204	0.11150	0.09526	0.08617	0.10841	0.12716	0.11143	0.08611	0.07233	0.07042
0.24406	0.12965	0.10902	0.09394	0.07598	0.10412	0.12325	0.11178	0.08509	0.07067	0.06933
0.25486	0.12727	0.10703	0.09218	0.07146	0.10016	0.11713	0.11204	0.08442	0.06900	0.06833
0.26607	0.12464	0.10480	0.08954	0.06644	0.09603	0.10710	0.11198	0.08357	0.06783	0.06667
0.27784	0.12274	0.10380	0.08866	0.06450	0.09174	0.09962	0.11178	0.08357	0.06717	0.06567
0.29007	0.12036	0.10231	0.08668	0.06241	0.08597	0.09163	0.11157	0.08442	0.06633	0.06483
0.30290	0.11798	0.10033	0.08492	0.06176	0.08168	0.08687	0.11143	0.08509	0.06633	0.06417
0.31623	0.11392	0.09784	0.08272	0.06079	0.07973	0.07573	0.11127	0.08577	0.06677	0.06333
0.33022	0.11202	0.09586	0.08096	0.05949	0.07211	0.07497	0.11113	0.08543	0.06703	0.06283
0.34475	0.10963	0.09337	0.07854	0.05755	0.07038	0.06617	0.10841	0.08458	0.06737	0.06242
0.35999	0.10773	0.09139	0.07634	0.05658	0.06221	0.06732	0.10571	0.08391	0.06763	0.06208
0.37584	0.10629	0.08890	0.07416	0.05497	0.05833	0.06460	0.10167	0.08306	0.06797	0.06067
0.39246	0.10534	0.08692	0.07238	0.05367	0.05635	0.06154	0.09763	0.08239	0.06823	0.05967
0.40973	0.10415	0.08443	0.06974	0.05270	0.05379	0.05882	0.09141	0.08168	0.06857	0.05833
0.42786	0.10320	0.08245	0.06886	0.05173	0.05280	0.05678	0.08635	0.08154	0.06883	0.05733
0.44668	0.10200	0.08152	0.06776	0.05076	0.05181	0.05304	0.07525	0.08137	0.06917	0.05567
0.46644	0.10058	0.07963	0.06600	0.04979	0.05066	0.05082	0.06885	0.08123	0.06943	0.05467
0.48697	0.09819	0.07772	0.06446	0.04826	0.04884	0.04794	0.06212	0.08107	0.06933	0.05383
0.50851	0.09629	0.07474	0.06314	0.04712	0.04686	0.04607	0.05774	0.08093	0.06867	0.05317
0.53088	0.09533	0.07276	0.06182	0.04640	0.04149	0.04284	0.05286	0.08025	0.06793	0.05217
0.55437	0.09486	0.07127	0.06094	0.04575	0.03688	0.04012	0.04881	0.07816	0.06767	0.05167
0.57876	0.09426	0.06991	0.05885	0.04519	0.03465	0.03638	0.04587	0.07528	0.06760	0.05058
0.60436	0.09379	0.06926	0.05687	0.04438	0.03366	0.03434	0.04453	0.07122	0.06760	0.05058
0.63096	0.09319	0.06829	0.05566	0.04349	0.03209	0.03391	0.04301	0.06665	0.06760	0.05150
0.65886	0.09200	0.06730	0.05522	0.04284	0.03077	0.03408	0.04216	0.06225	0.06760	0.05217
0.68786	0.08913	0.06606	0.05357	0.04228	0.02970	0.03447	0.04090	0.05667	0.06760	0.05333
0.71828	0.08818	0.06531	0.05291	0.04146	0.02871	0.03465	0.03888	0.05261	0.06753	0.05467
0.74989	0.08711	0.06442	0.05159	0.04050	0.02780	0.03417	0.03493	0.04804	0.06583	0.05617
0.78306	0.08649	0.06382	0.05071	0.03969	0.02731	0.03179	0.03223	0.04500	0.06250	0.05683
0.81752	0.08566	0.06345	0.05005	0.03872	0.02690	0.02720	0.02870	0.04035	0.05600	0.05758
0.85368	0.08518	0.06345	0.04939	0.03839	0.02640	0.02499	0.02601	0.03679	0.05067	0.05775
0.89125	0.08544	0.06307	0.04829	0.03783	0.02566	0.02320	0.02306	0.03256	0.04567	0.05700
0.93067	0.08612	0.06283	0.04763	0.03702	0.02533	0.02218	0.02188	0.03020	0.04167	0.05583

0.97163	0.08705	0.06184	0.04728	0.03614	0.02467	0.02150	0.02185	0.02833	0.03783	0.05367
1.01460	0.08721	0.06059	0.04697	0.03532	0.02434	0.02090	0.02199	0.02597	0.03500	0.04967
1.05925	0.08641	0.05992	0.04657	0.03460	0.02393	0.02031	0.02207	0.02427	0.03200	0.04558
1.10610	0.08590	0.05992	0.04627	0.03427	0.02359	0.01991	0.02146	0.02275	0.03017	0.04225
1.15478	0.08587	0.06133	0.04569	0.03387	0.02321	0.01933	0.01934	0.02098	0.02867	0.03833
1.20586	0.08619	0.06233	0.04503	0.03354	0.02299	0.01899	0.01695	0.01996	0.02750	0.03583
1.25893	0.08656	0.06084	0.04480	0.03314	0.02269	0.01853	0.01525	0.01919	0.02617	0.03242
1.31460	0.08675	0.06084	0.04477	0.03265	0.02236	0.01823	0.01471	0.01871	0.02517	0.02975
1.37246	0.08699	0.05987	0.04472	0.03193	0.02195	0.01783	0.01427	0.01788	0.02433	0.02692
1.43316	0.08718	0.06022	0.04472	0.03161	0.02175	0.01746	0.01401	0.01686	0.02383	0.02475
1.49624	0.08890	0.06084	0.04477	0.03120	0.02146	0.01707	0.01367	0.01533	0.02357	0.02258
1.56241	0.08928	0.06124	0.04480	0.03088	0.02114	0.01666	0.01326	0.01428	0.02297	0.02075
1.63117	0.08911	0.06159	0.04485	0.03030	0.02089	0.01627	0.01293	0.01321	0.02117	0.01923
1.70331	0.08891	0.06209	0.04488	0.02991	0.02076	0.01610	0.01270	0.01223	0.01880	0.01810
1.77828	0.08294	0.06270	0.04504	0.02950	0.02054	0.01599	0.01230	0.01125	0.01637	0.01678
1.85693	0.07960	0.06305	0.04538	0.02918	0.02035	0.01593	0.01207	0.01068	0.01473	0.01598
1.93865	0.07555	0.06330	0.04578	0.02898	0.02010	0.01578	0.01184	0.01043	0.01302	0.01507
2.02439	0.07150	0.06330	0.04582	0.02888	0.01993	0.01564	0.01170	0.01037	0.01202	0.01467
2.11349	0.06658	0.06320	0.04565	0.02854	0.01977	0.01547	0.01153	0.01028	0.01127	0.01475
2.20696	0.05491	0.06211	0.04530	0.02821	0.01963	0.01537	0.01139	0.01010	0.01083	0.01492
2.30409	0.02484	0.05835	0.04504	0.02781	0.01947	0.01530	0.01123	0.00985	0.01023	0.01377
2.40600	0.00759	0.05612	0.04556	0.02771	0.01940	0.01530	0.01113	0.00979	0.00990	0.01140
2.51189	0.00069	0.05202	0.04565	0.02783	0.01940	0.01525	0.01104	0.00973	0.00943	0.01015
2.62298	0.00005	0.04731	0.04499	0.02777	0.01927	0.01508	0.01098	0.00961	0.00910	0.00938
2.73842		0.03452	0.04246	0.02766	0.01908	0.01470	0.01093	0.00936	0.00850	0.00860
2.85953		0.01695	0.04092	0.02749	0.01894	0.01443	0.01089	0.00926	0.00823	0.00820
2.98538		0.00276	0.03883	0.02726	0.01881	0.01432	0.01084	0.00914	0.00772	0.00778
3.11742		0.00031	0.03663	0.02770	0.01888	0.01430	0.01080	0.00914	0.00751	0.00752
3.25462			0.02745	0.02849	0.01904	0.01425	0.01075	0.00914	0.00745	0.00717
3.39856			0.01298	0.02877	0.01918	0.01419	0.01071	0.00914	0.00741	0.00687
3.54813			0.00200	0.02802	0.01933	0.01420	0.01066	0.00914	0.00733	0.00653
3.70506			0.00020	0.02668	0.01947	0.01422	0.01062	0.00914	0.00727	0.00627
3.86812				0.02561	0.01963	0.01423	0.01047	0.00906	0.00717	0.00607
4.03919				0.02519	0.01950	0.01425	0.01033	0.00903	0.00707	0.00587
4.21696				0.02256	0.01888	0.01426	0.01019	0.00900	0.00693	0.00574
4.40347				0.01526	0.01861	0.01428	0.01017	0.00886	0.00687	0.00571
4.59727				0.00403	0.01812	0.01429	0.01016	0.00870	0.00692	0.00567
4.80059				0.00055	0.01733	0.01431	0.01014	0.00863	0.00692	0.00562
5.01187				0.00001	0.01660	0.01432	0.01013	0.00863	0.00680	0.00549
5.23353					0.01601	0.01431	0.01011	0.00863	0.00657	0.00544
5.46387					0.01248	0.01427	0.01003	0.00863	0.00650	0.00538
5.70552					0.00588	0.01407	0.01003	0.00863	0.00650	0.00532
5.95662					0.00060	0.01357	0.01026	0.00856	0.00649	0.00523
6.22007					0.00003	0.01312	0.01076	0.00846	0.00647	0.00517
6.49382						0.01183	0.01085	0.00839	0.00646	0.00508
6.78102						0.00794	0.01059	0.00856	0.00644	0.00502
7.07946						0.00142	0.00992	0.00863	0.00642	0.00496

(continued on p. 22)

TABLE 4 *(continued)*

Pulse height	Absolute differential efficiencies for neutron energies of									
	6.017 MeV	7.037 MeV	8.029 MeV	10.000 MeV	11.980 MeV	14.007 MeV	16.055 MeV	17.805 MeV	19.907 MeV	21.809 MeV
7.39256						0.00011	0.00988	0.00863	0.00641	0.00496
7.71791							0.00875	0.00849	0.00642	0.00499
8.05925							0.00484	0.00829	0.00644	0.00500
8.41395							0.00061	0.00772	0.00645	0.00500
8.78607							0.00003	0.00717	0.00639	0.00499
9.17276								0.00336	0.00617	0.00498
9.57845								0.00057	0.00590	0.00496
10.00000								0.00001	0.00537	0.00492
10.44227									0.00355	0.00483
10.90184									0.00052	0.00472
11.38400									0.00002	0.00396
11.88502										0.00143
12.41066										0.00017

point on the proton-recoil plateau to the area of the calculation above the same pulse height. Each final experimental curve corresponds to a pulse-height distribution from a plane parallel beam of monoenergetic neutrons incident on the curved face of a 4.60- by 4.65-cm-dia. scintillator, perpendicular to its axis, and normalized to one neutron incident on the NE-213. The resulting response functions are illustrated in fig. 3, along with a ^{22}Na pulse-height spectrum used for gain calibration. The error bars shown at the lower left part of the figure indicate the degree of uncertainty in the pulse-shape discriminator corrections. For example, the correction function shown in fig. 4 was assumed to hold for carbon recoils and alpha particles that become important above 7-MeV incident neutron energy. The correction functions for these events are likely to be different from that for proton recoils.

The absolute differential efficiencies (response functions) for neutrons of 20 energies shown in fig. 3 are also given in table 4. In both cases the 10-MeV response does not represent the results of a measurement. In the region of the proton-recoil plateau this 10-MeV response is the result of a Monte Carlo calculation. Below this plateau the curve was obtained with a hand interpolation, using the measured 8- and 12-MeV responses, since the calculation is not reliable below the proton-recoil plateau; the carbon cross sections, obtained mostly by extrapolation from other energies, do not match the data at 8 or 12 MeV.

For convenience in time-of-flight work, the detector efficiency versus bias (integral bias efficiency) is given in table 5. If an NE-213 scintillator is used with a pulse-shape discrimination circuit of the type presented here, corrections below about 0.1 light units would have to be made for losses in the circuit. But for bias settings higher than this, a well-adjusted discriminator circuit should require no correction (fig. 4). For a NE-211 scintillator, with which good pulse-shape discrimination is not feasible, table 5 may be used as is. A small correction may be applied for detecting 4.43-MeV gamma rays from ^{12}C(n,n')^{12}C reactions in the scintillator. However, this correction is only about 2.5% at the 8-MeV peak in the inelastic cross section for this scintillator size. In any case, the discriminator must produce a sharp cutoff such as would be obtained from a discriminator operating on a slow amplifier output. If a sharp cutoff is not produced, then the problem of an effective bias will make the use of table 5 more difficult.

8. Applications

The present set of 20 calibrations and one inter-

TABLE 5

Absolute integral counting efficiency versus bias setting in pulse-height units defined by table 3. The efficiency is obtained by integration of the data of table 4 above the bias level, and represents the counting efficiency at the given bias setting, averaged over the scintillator's cross-sectional area.

	Absolute differential efficiencies for neutron energies of										
Pulse height	0.201 MeV	0.322 MeV	0.427 MeV	0.617 MeV	0.904 MeV	1.205 MeV	1.613 MeV	2.233 MeV	3.238 MeV	4.236 MeV	4.919 MeV
0.01540	0.10839	0.39654	0.46704	0.47870	0.46131	0.43763	0.40054	0.36246	0.31311	0.27626	0.25724
0.01995	0.02147	0.25949	0.39167	0.43793	0.43667	0.41957	0.38683	0.35175	0.30512	0.27086	0.25257
0.02585	0.00168	0.10224	0.28325	0.38917	0.40898	0.40016	0.37296	0.34127	0.29828	0.26584	0.24853
0.03350	0.00004	0.01593	0.13706	0.32501	0.37699	0.37869	0.35877	0.33056	0.29178	0.26080	0.24445
0.04340		0.00061	0.02975	0.23186	0.33685	0.35393	0.34294	0.31923	0.28469	0.25563	0.24016
0.05623			0.00171	0.11315	0.28400	0.323 5	0.32385	0.30667	0.27656	0.25002	0.23558
0.07286			0.00001	0.02297	0.21132	0.28603	0.30019	0.29209	0.26733	0.24389	0.23054
0.09441				0.00071	0.12031	0.23693	0.27144	0.27571	0.25700	0.23716	0.22487
0.12232					0.03685	0.16982	0.23635	0.25640	0.24536	0.22941	0.21847
0.15849					0.00126	0.09007	0.19108	0.23286	0.23138	0.22020	0.21095
0.20535						0.01958	0.13051	0.20421	0.21468	0.20936	0.20225
0.26607						0.00013	0.06114	0.16681	0.19447	0.19646	0.19201
0.34475							0.00656	0.11679	0.17001	0.18026	0.17997
0.44668								0.05475	0.13946	0.16108	0.16530
0.57876								0.00394	0.09901	0.13762	0.14753
0.74989									0.05015	0.10838	0.12484
0.97163									0.00476	0.06998	0.09639
1.25893										0.02468	0.05826
1.63117										0.00002	0.01527

	Absolute differential efficiencies for neutron energies of									
Pulse height	6.017 MeV	7.037 MeV	8.029 MeV	10.000 MeV	11.980 MeV	14.007 MeV	16.055 MeV	17.805 MeV	19.907 MeV	21.809 MeV
0.01540	0.23155	0.20803	0.19722	0.17811	0.16919	0.15920	0.15680	0.16251	0.16343	0.16772
0.01995	0.22783	0.20485	0.19231	0.17415	0.16598	0.15589	0.15400	0.15910	0.15901	0.16100
0.02585	0.22451	0.20206	0.18850	0.17146	0.16402	0.15371	0.15204	0.15672	0.15596	0.15649
0.03350	0.22124	0.19932	0.18515	0.16900	0.16221	0.15203	0.15036	0.15471	0.15343	0.15292
0.04340	0.21781	0.19654	0.18189	0.16658	0.16031	0.15040	0.14869	0.15285	0.15119	0.14972
0.05623	0.21405	0.19351	0.17813	0.16381	0.15799	0.14858	0.14671	0.15083	0.14907	0.14680
0.07286	0.20990	0.19015	0.17350	0.16038	0.15424	0.14597	0.14395	0.14813	0.14680	0.14408
0.09441	0.20526	0.18645	0.16873	0.15615	0.14908	0.14235	0.14043	0.14479	0.14418	0.14140
0.12232	0.19999	0.18228	0.16490	0.15121	0.14249	0.13837	0.13661	0.14099	0.14118	0.13862
0.15849	0.19402	0.17731	0.16062	0.14574	0.13511	0.13380	0.13256	0.13663	0.13775	0.13544
0.20535	0.18720	0.17148	0.15571	0.13989	0.12830	0.12800	0.12744	0.13191	0.13383	0.13169
0.26607	0.17915	0.16467	0.14989	0.13450	0.12163	0.12038	0.12069	0.12657	0.12942	0.12736

(continued on p. 24)

TABLE 5 *(continued)*

Pulse height	Absolute differential efficiencies for neutron energies of									
	6.017 MeV	7.037 MeV	8.029 MeV	10.000 MeV	11.980 MeV	14.007 MeV	16.055 MeV	17.805 MeV	19.907 MeV	21.809 MeV
0.34475	0.16985	0.15675	0.14318	0.12959	0.11508	0.11336	0.11191	0.11991	0.12415	0.12228
0.44668	0.15905	0.14782	0.13573	0.12405	0.10918	0.10695	0.10193	0.11147	0.11721	0.11617
0.57876	0.14615	0.13778	0.12729	0.11772	0.10313	0.10081	0.09396	0.10085	0.10814	0.10912
0.74989	0.13047	0.12622	0.11782	0.11033	0.09775	0.09489	0.08671	0.08997	0.09657	0.10018
0.97163	0.11141	0.11214	0.10684	0.10177	0.09188	0.08892	0.08062	0.08147	0.08480	0.08757
1.25893	0.08659	0.09462	0.09355	0.09184	0.08505	0.08314	0.07473	0.07471	0.07572	0.07499
1.63117	0.05395	0.07204	0.07689	0.07999	0.07692	0.07660	0.06947	0.06842	0.06669	0.06535
2.11349	0.01498	0.04179	0.05503	0.06580	0.06708	0.06891	0.06357	0.06297	0.05908	0.05738
2.73842		0.00672	0.02668	0.04832	0.05491	0.05936	0.05657	0.05680	0.05278	0.04973
3.54813			0.00035	0.02571	0.03953	0.04774	0.04781	0.04935	0.04648	0.04354
4.59727				0.00094	0.01937	0.03279	0.03691	0.03988	0.03904	0.03724
5.95662					0.00017	0.01341	0.02318	0.02813	0.02995	0.02979
7.71791							0.00494	0.01309	0.01860	0.02088
10.00000									0.00426	0.00950

polated response for monoenergetic neutrons with energies between 0.2 and 22 MeV have been carried out to provide a reliable response matrix. The response matrix generally consists of a large number of response functions that can be obtained by interpolating between the 21 curves of fig. 3. This matrix must be accurately known when it is used with the method of neutron spectroscopy based on unfolding a pulse-height distribution to obtain an energy spectrum[10-12]), because small errors in the matrix can result in much larger errors in the unfolded energy spectrum. The responses presented in fig. 3 and table 4 should be a considerable improvement on past efforts[7,13,14]) because of the unique combination of measurement and calculation used here and because of the large range in pulse height achieved with the measuring techniques employed.

Integration of the calibrations and the interpolated response above some bias level L_b results in a set of efficiency values which are useful in time-of-flight measurements[15,16]). These values, presented in table 5, can be used directly with the present size of scintillator. Although the size and shape of this scintillator are far from optimum for most time-of-flight applications, the calibration results are nevertheless very useful: any other scintillator can be directly and rapidly cross-calibrated against the present one if a pulsed, broad-spectrum neutron source is available, such as from an electron linear accelerator with lead target[16]). With the resultant time-of-flight separation of neutron energies, the present spectrometer can also be used as an absolute neutron flux monitor in calibrating other detectors. The greatest accuracy is achieved by biasing the present "standard" detector in the proton-recoil plateau. In this way, Monte Carlo calibrations to which the present pulse-height distributions were normalized are utilized most directly.

We express our appreciation to J. R. Drischler for his tireless efforts in processing the data, to R. W. Peelle for many helpful discussions, and to F. C. Maienschein for unfailing encouragement, interest and support.

References

1) R. E. Textor and V. V. Verbinski, 05S; A Monte Carlo code for calculating pulse height distributions due to monoenergetic neutrons incident on organic scintillators, Oak Ridge National Laboratory Report ORNL-4160 (1968). Available from Clearinghouse for Federal Scientific and Technical Information, National Bureau of Standards, U.S. Dept. of Commerce, Springfield, Virginia 22151, U.S.A.

2) W. R. Burrus and V. V. Verbinski, Nucl. Instr. and Meth., in press.

3) M. Forté, A. Konsta and C. Maranzana, Proc. IAEA Conf. *Nuclear electronics*, Belgrade (IAEA, Vienna, 1962).

4) C. D. Swartz and G. E. Owen, *Fast neutron physics* **1** (ed.

J.B. Marion and J.L. Fowler; Interscience, New York 1960) 211.
[5]) T. A. Love, R. T. Santoro, R. W. Peelle and N. W. Hill, Rev. Sci. Instr. **39** (1968) 541.
[6]) M. D. Goldberg, V. M. May and J. R. Stehn, Angular distribution in neutron-induced reactions, $Z = 1$ to 22; Brookhaven National Laboratory Report BNL-400, 2nd ed., **1** (1962).
[7]) V. V. Verbinski, J. C. Courtney, W. R. Burrus and T. A. Love, Proc. Amer. Nucl. Soc., Special session *Fast neutron spectroscopy*, San Francisco (Dec., 1964) Shielding Division Report ANS-SD-2 (unpublished) 189.
[8]) J. D. Kington, J. K. Bair, H. O. Cohn and H. B. Willard, Phys. Rev. **99** (1955) 1393.
[9]) K. F. Flynn, L. E. Glendenin, E. P. Steinberg and P. M. Wright, Nucl. Instr. and Meth. **27** (1964) 13. (The prescription: the half-height, at the Compton edge of the pulse-height distribution, is 4% above the Compton-edge electron energy.)
[10]) V. V. Verbinski, F. G. Perey and J. K. Dickens, Phys. Rev. **170** (1968) 916.
[11]) V. V. Verbinski and W. R. Burrus, Direct and compound-nucleus neutrons from 14- to 18-MeV protons on ^{9}Be, ^{14}N, ^{27}Al, ^{56}Fe, ^{115}In, ^{181}Ta and ^{208}Pb, and from 33-MeV bremstrahlung on ^{27}Al, ^{206}Pb and ^{209}Bi, Phys. Rev., in press.
[12]) C. E. Clifford et al., Nucl. Sci. Eng. **27** (1967) 299.
[13]) R. Batchelor et al., Nucl. Instr. and Meth. **13** (1961) 70.
[14]) B. Brunfelter, J. Kockum and H. O. Zetterström, Nucl. Instr. and Meth. **40** (1966) 84.
[15]) V. V. Verbinski and J. C. Courtney, Nuclear Physics **73** (1965) 398.
[16]) V. V. Verbinski, J. C. Courtney and N. Betz, Nucl. Instr. and Meth. **52** (1967) 181.